

## ATMOSPHERIC NEUTRINO OSCILLATIONS IN MACRO

GIORGIO GIACOMELLI and MIRIAM GIORGINI

*Dept. of Physics, University of Bologna, V.le C. Berti Pichat 6/2  
Bologna, I-40127, Italy*

E-mail: giorgio.giacomelli@bo.infn.it , miriam.giorgini@bo.infn.it

Invited paper at NO-VE, Int. Workshop on Neutrino Oscillations in Venice,  
Venice, Italy, 24-26 July 2001.

## Abstract

In this paper we first give a short overview of the MACRO detector which was operational at the Gran Sasso Laboratory from 1989 till the end of 2000. Then we present and discuss the results on atmospheric muon neutrino oscillations, concerning medium ( $\sim 4$  GeV) and high ( $\sim 50$  GeV) energy data. Using the Multiple Coulomb Scattering of muons inside the lower part of the detector, estimates of neutrino energies were made for the high energy sample. The data on angular distributions, absolute flux and  $L/E_\nu$  distributions favour  $\nu_\mu \longleftrightarrow \nu_\tau$  oscillations with maximal mixing and  $\Delta m^2 = 2.5 \cdot 10^{-3}$  eV<sup>2</sup>.

## 1 Introduction

MACRO was a large multipurpose underground detector designed primarily to search for rare particles in the penetrating cosmic radiation. Though it was optimized to search for the supermassive magnetic monopoles predicted by Grand Unified Theories (GUT) of the electroweak and strong interactions, the MACRO research program included a wide range of topics in areas of astrophysics, nuclear and particle physics and cosmic ray physics. In particular it planned to study atmospheric neutrinos via the detection of upgoing muons produced in charge current (CC) interactions of  $\nu_\mu$  in the rock below the detector and inside its lower part.

A high energy primary cosmic ray, proton or nucleus, interacts in the upper atmosphere producing a large number of pions and kaons, which decay yielding muons and muon neutrinos; also the muons decay yielding muon and electron neutrinos, Fig: 1. The ratio of the numbers of muon to electron neutrinos is about 2, and  $N_\nu/N_{\bar{\nu}} \simeq 1$ . These neutrinos are produced in a spherical surface at about 20 km above ground and they proceed at high speed towards the Earth. An underground detector is “illuminated” by a flux of neutrinos from all directions.

At low energies,  $E_\nu \sim 1$  GeV, the numbers of atmospheric neutrinos predicted by different authors differ by about 20 ÷ 30% [1]; at higher energies,  $E_\nu > 10$  GeV, the predictions are more reliable, with an estimated systematic uncertainty of about 15% [2], almost one half of the uncertainty at low energies. However the predicted relative rates of  $\nu_\mu$  to  $\nu_e$  and the shapes of the zenith angle distributions are affected by considerably lower systematic errors. Other sources of systematic uncertainties arise from the knowledge of the neutrino-nucleon cross sections and from the propagation of muons and electrons in different materials.

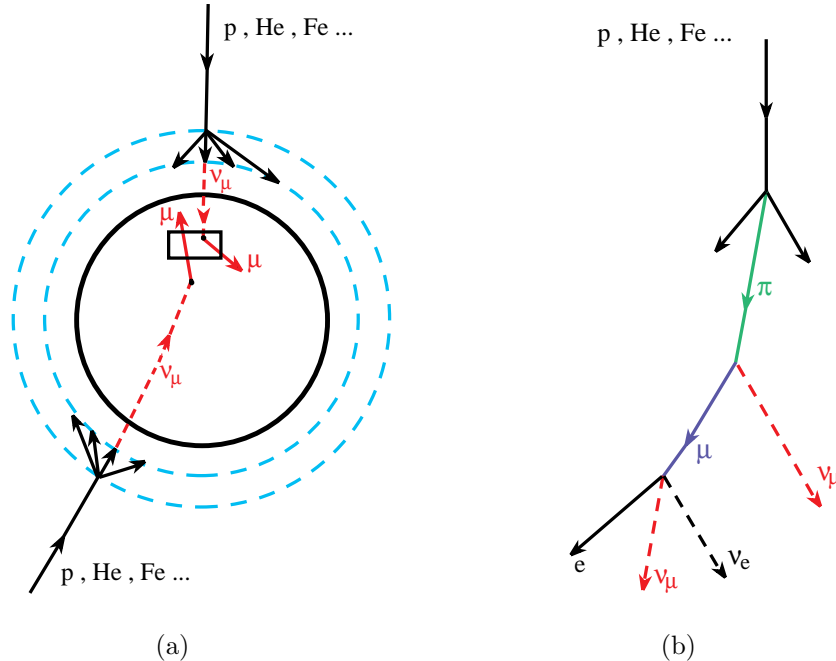


Figure 1: (a) Illustration of the production, travel and interactions of atmospheric muon neutrinos; (b) interaction of a primary cosmic ray, production of pions (and kaons) and their decays leading to the atmospheric  $\nu_e$ ,  $\nu_\mu$ .

Several large underground detectors studied atmospheric neutrinos, mainly via charged current interactions, where a  $\nu_\mu$  gives rise to a  $\mu^-$ , and thus to a track, and a  $\nu_e$  yields an  $e^-$  and thus to an electromagnetic shower.

The early water Cherenkov detectors IMB [3] and Kamiokande [4] reported anomalies in the double ratio of muon to electron neutrinos integrated over all zenith angles, while the tracking calorimeters NUSEX [5] and Frejus [6], and the Baksan [7] scintillator detector did not find any deviation, see Fig: 2.

Later the Soudan 2 [8], MACRO [9] and SuperKamiokande [10] detectors reported a deficit in the  $\nu_\mu$  flux with respect to the MC predictions and a distortion of the angular distributions, while the  $\nu_e$  flux and angular distributions agree with MC. These features may be explained in terms of  $\nu_\mu \longleftrightarrow \nu_\tau$  oscillations.

Atmospheric neutrinos are well suited for the study of neutrino oscillations, since they have energies from a fraction of a GeV up to more than 100 GeV and they may travel distances  $L$  from few tens of km up to 13000 km; thus the  $L/E_\nu$  values range from  $\sim 1$  km/GeV to more than  $10^4$  km/GeV.

In the following, we shall briefly recall neutrino oscillation formulae and the main features of the MACRO detector, then we shall discuss the main results of MACRO, including the ratio of vertical to horizontal muons which favour  $\nu_\mu \longleftrightarrow \nu_\tau$  oscillations and the estimates of neutrino energies by multiple coulomb scattering of muons, which allows the study of the  $L/E_\nu$  distribution. We shall conclude with a short discussion and by recalling briefly other neutrino studies by MACRO.

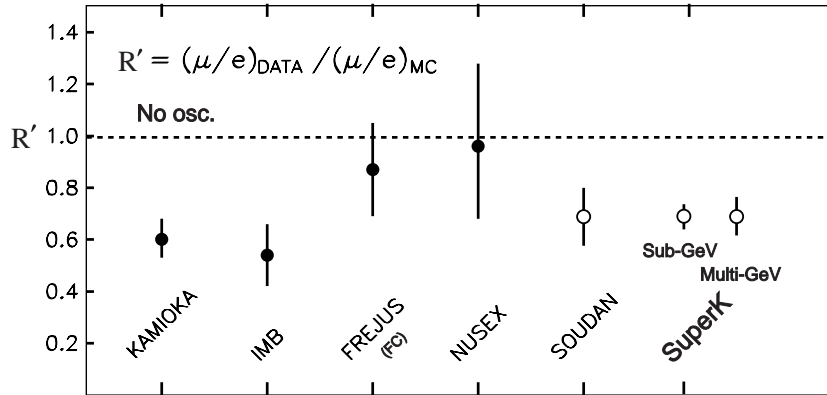


Figure 2: Double ratios  $R'$  measured by several atmospheric neutrino experiments.

## 2 Neutrino oscillations

If neutrinos have non-zero masses, one has to consider the neutrino *weak flavour eigenstates*  $\nu_e, \nu_\mu, \nu_\tau$  and the *mass eigenstates*  $\nu_1, \nu_2, \nu_3$ . The weak flavour eigenstates  $\nu_l$  are linear combinations of the mass eigenstates  $\nu_m$  through the elements of the mixing matrix  $U_{lm}$ :

$$\nu_l = \sum_{m=1}^3 U_{lm} \nu_m \quad (1)$$

If the mixing angles are small, one would have  $\nu_e \sim \nu_1, \nu_\mu \sim \nu_2, \nu_\tau \sim \nu_3$ . If the mixing angles are large, the flavour eigenstates are well separated from those of mass.

In the simple case of only two flavour eigenstate neutrinos ( $\nu_\mu, \nu_\tau$ ) which oscillate with two neutrino mass eigenstates ( $\nu_2, \nu_3$ ) one has

$$\begin{cases} \nu_\mu = \nu_2 \cos \theta_{23} + \nu_3 \sin \theta_{23} \\ \nu_\tau = -\nu_2 \sin \theta_{23} + \nu_3 \cos \theta_{23} \end{cases} \quad (2)$$

where  $\theta_{23}$  is the mixing angle. In this case one may easily compute the following expression for the survival probability of a  $\nu_\mu$  beam (disappearance experiment):

$$P(\nu_\mu \rightarrow \nu_\mu) = 1 - \sin^2 2\theta_{23} \sin^2 \left( \frac{E_2 - E_1 t}{2} \right) = 1 - \sin^2 2\theta_{23} \sin^2 \left( \frac{1.27 \Delta m^2 \cdot L}{E_\nu} \right) \quad (3)$$

where  $\Delta m^2 = m_3^2 - m_2^2$ , and  $L$  is the distance travelled by the neutrino from production to the detection point. The probability for the initial  $\nu_\mu$  to oscillate into a  $\nu_\tau$  is (appearance experiment):

$$P(\nu_\mu \rightarrow \nu_\tau) = 1 - P(\nu_\mu \rightarrow \nu_\mu) = \sin^2 2\theta_{23} \sin^2 \left( \frac{1.27 \Delta m^2 \cdot L}{E_\nu} \right) \quad (4)$$

In a disappearance experiment one measures only  $P(\nu_\mu \rightarrow \nu_\mu)$  as a function of  $E_\nu$  and  $L$ , or of  $L/E_\nu$ . Only disappearance experiments have been performed until now. For atmospheric neutrinos the parameters  $\theta_{23}$  and  $\Delta m^2$  may be determined from the variation of  $P(\nu_\mu \rightarrow \nu_\mu)$  as a function of the zenith angle  $\Theta$ , or from the variation in  $L/E_\nu$ . In future appearance experiments, one would try to observe a neutrino, for example  $\nu_\tau$ , not produced in  $\pi, K$  decays.

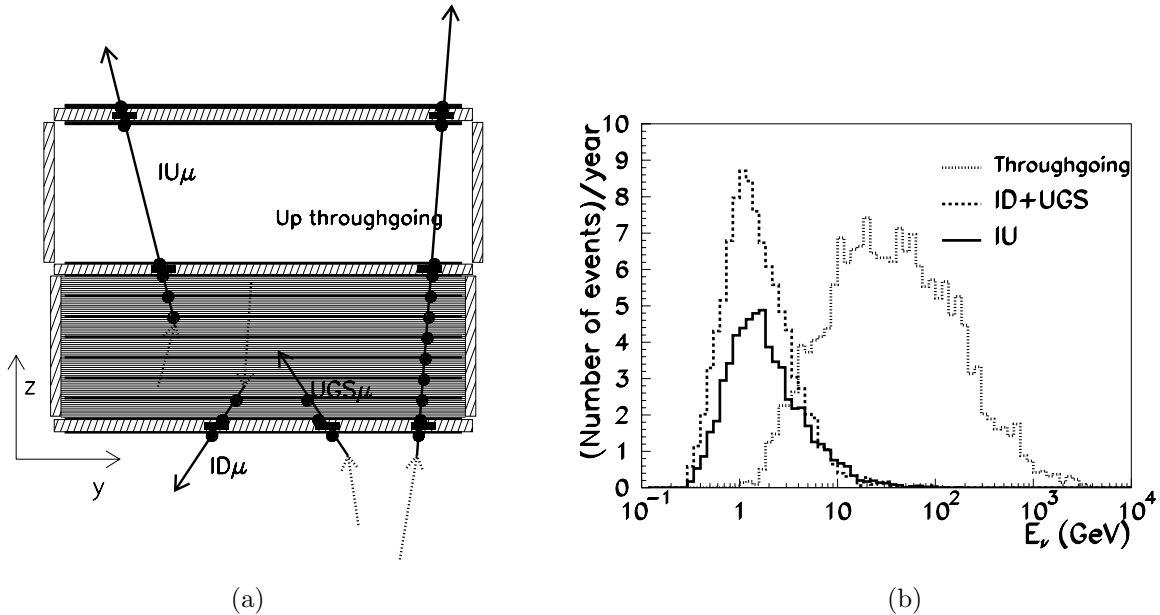


Figure 3: (a) Vertical section of the MACRO detector. Event topologies induced by  $\nu_\mu$  interactions in or around the detector: IU = semicontained Internal Upgoing  $\mu$ ; ID = Internal Downgoing  $\mu$ ; UGS = Upgoing Stopping  $\mu$ ; Upthroughgoing = upward throughgoing  $\mu$ . The black circles indicate the streamer tube hits and the black boxes the scintillator hits. (b) MC simulated distributions of the parent neutrino energies, assuming no oscillations, giving rise to the different topologies of muon events detectable by MACRO. The distributions are normalized to one year of data taking.

### 3 The MACRO experiment

The MACRO detector was located in Hall B of the Gran Sasso Laboratory, under a minimum rock overburden of  $3150 \text{ hg/cm}^2$  which reduces the atmospheric muon flux by a factor  $\sim 5 \cdot 10^5$ . It was a large rectangular box,  $76.6\text{m} \times 12\text{m} \times 9.3\text{m}$ , divided longitudinally in six supermodules and vertically in a lower part (4.8 m high) and an upper part (4.5 m high) [11] (Fig: 3a). It had three types of detectors which gave redundancy of informations: liquid scintillation counters, limited streamer tubes and nuclear track detectors. This last detector was used only for new particle searches.

For muon and for neutrino physics and astrophysics studies, the streamer tubes were used for muon tracking and the liquid scintillation counters for fast timing. The lower part of the detector was filled with trays of crushed rock absorbers alternating with streamer tube planes; the upper part was open and contained the electronics.

There were 10 horizontal planes of streamer tubes in the bottom half of the detector, and 4 planes at the top, all with wire and  $27^\circ$  stereo strip readouts. Six vertical planes of streamer tubes and one layer of scintillators covered each side of the detector. The scintillator system consisted of three layers of horizontal counters, and of the mentioned vertical layer along the sides of the detector. One thus had a closed box structure with openings only in the upper part of the front and back ends.

The time and space resolutions for muons in a scintillation counter were about 500 ps and 11 cm, respectively, while in the streamer tube system they were about 100 ns and 1 cm, respectively. The combination of the informations from the streamer tubes and from the scintillators allowed tracking with a precision of 1 cm over path lengths of several meters,

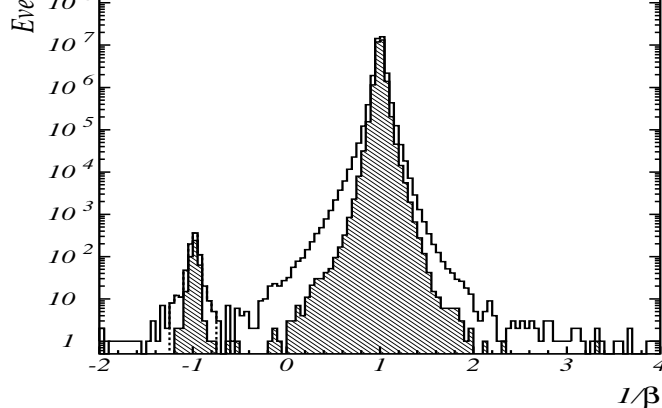


Figure 4:  $1/\beta$  distributions for throughgoing (downgoing and upgoing) muons for the runs with the complete detector. The shaded areas concern muons crossing 3 scintillation counters, while the open histogram concerns muons crossing 2 or 3 counters. Two vertical dotted lines delimit the range  $-1.25 \leq 1/\beta \leq -0.75$  of upthroughgoing muons. There are  $\sim 3.5 \cdot 10^7$  downgoing muons with  $1/\beta \sim 1$  and 782 (before subtraction of background) upgoing muons with  $1/\beta \sim -1$ .

and timing with a precision of 500 ps. The detector provided a total acceptance  $S\Omega \simeq 10000$   $\text{m}^2$  sr for an isotropic flux of particles.

Fig: 3a is a vertical section of the detector; it shows a general view of the detector and gives also a sketch of the different topologies of detected neutrino-induced muon events used to study neutrino oscillations: Upthroughgoing muons, Internal Upgoing muons (IU), Upgoing Stopping muons (UGS) and Internal Downgoing muons (ID). Fig: 3b shows the parent neutrino energy distributions obtained from Monte Carlo calculations for the event topologies detectable in MACRO.

The *Upthroughgoing muons* (with  $E_\mu > 1$  GeV) come from interactions in the rock below the detector of muon neutrinos with an average energy  $\langle E_\nu \rangle \sim 50$  GeV. The tracking is performed with streamer tubes hits; the time information, provided by scintillation counters, allows the determination of the direction (versus) by the time-of-flight (T.o.F.) method. If the atmospheric neutrino anomalies are due to neutrino oscillations, one expects a muon flux reduction depending on the zenith angle.

The *semicontained upgoing muons* (IU) come from  $\nu_\mu$  interactions inside the lower apparatus. Since two scintillation counters are intercepted, the T.o.F. method is applied to identify the upward going muons. The average parent neutrino energy for these events is  $\sim 4$  GeV. If the atmospheric neutrino anomalies are the results of  $\nu_\mu$  oscillations with maximal mixing and  $10^{-3} < \Delta m^2 < 10^{-2}$   $\text{eV}^2$ , one expects a reduction of about a factor of two in the flux of IU events, without any distortion in the shape of the angular distribution.

The *up stopping muons* (UGS) are due to  $\nu_\mu$  interactions in the rock below the detector yielding upgoing muon tracks stopping in the detector; the *semicontained downgoing muons* (ID) are due to  $\nu_\mu$  induced downgoing tracks with vertex in the lower MACRO. The events are found by means of topological criteria; the lack of time information prevents to distinguish between the two subsamples. An almost equal number of UGS and ID events is expected. In case of oscillations, a similar reduction in the flux of the up stopping events and of the semicontained upgoing muons is expected; no reduction is instead expected for the semicontained downgoing events (which come from neutrinos which travelled  $\sim 20$  km).

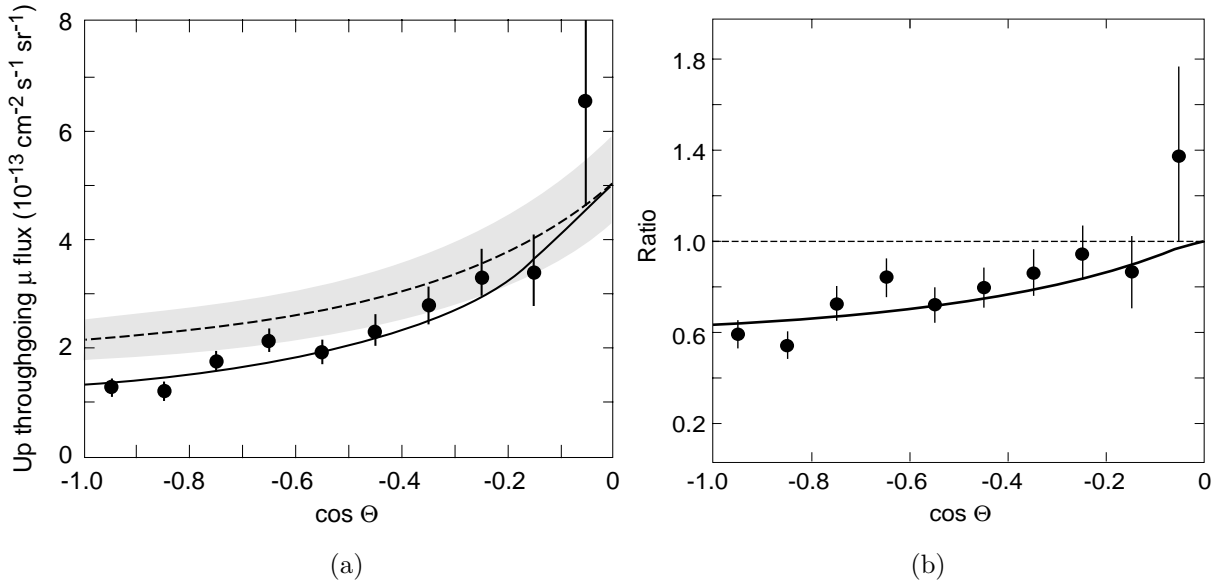


Figure 5: (a) Zenith distribution of the upthroughgoing muons (809 events, background subtracted). The data (black points) have statistical and systematic errors added in quadrature. The shaded region indicates the theoretical scale error band of  $\pm 17\%$  (see text). The solid line is the fit to an oscillated flux with maximal mixing and  $\Delta m^2 = 2.5 \cdot 10^{-3} \text{ eV}^2$ . (b) Zenith distribution of the ratio of measured upgoing muons over the expected ones with no oscillations (black points with statistical and systematic errors in quadrature). The solid line is the same ratio computed for oscillations; the dotted line corresponds to no oscillations.

## 4 High energy events

The data were collected during the running period from March 1989 to April 1994 with the detector under construction and during the runs with the complete detector from 1994 until December 2000 (livelime 5.52 yrs). Since the total livelime normalized to the full configuration is 6.16 yrs, the statistics is largely dominated by the full detector run. The analysis of a data sample of more than 40 million atmospheric downgoing muons achieved a rejection factor of  $\sim 10^{-7}$  which includes background caused by showering events and radioactivity in coincidence with muons.

We studied many sources of possible background: (i) low energy upgoing particles (mainly pions) induced by undetected downgoing muons in the rock surrounding the detector [12]. This source of background is reduced to 1% requiring that more than  $200 \text{ gr/cm}^2$  of material be crossed in the lower part of MACRO; (ii) we excluded a region in the azimuthal angle from  $-30^\circ$  to  $120^\circ$  for nearly horizontal upgoing muons due to insufficient rock overburden; (iii) for muons crossing 3 scintillation counters a linear fit of the times as a function of the path length is performed and a cut is applied on the  $\chi^2$ ; (iv) further minor cuts are applied to events crossing 2 counters.

Muons traveling downwards have  $1/\beta \sim +1$ , upwardgoing muons have  $1/\beta \sim -1$ . The  $1/\beta$  distribution for the sample collected with the full detector is shown in Fig: 4. We selected upwardgoing muons requiring  $-1.25 \leq 1/\beta \leq -0.75$ ; we found 863 events, of which 809 events remain after subtracting the background.

In the upgoing muon simulation the neutrino flux computed by the Bartol group [13] was used. The cross sections for the neutrino interactions was calculated using the deep inelastic parton distributions [14]. The muon propagation to the detector was computed using the

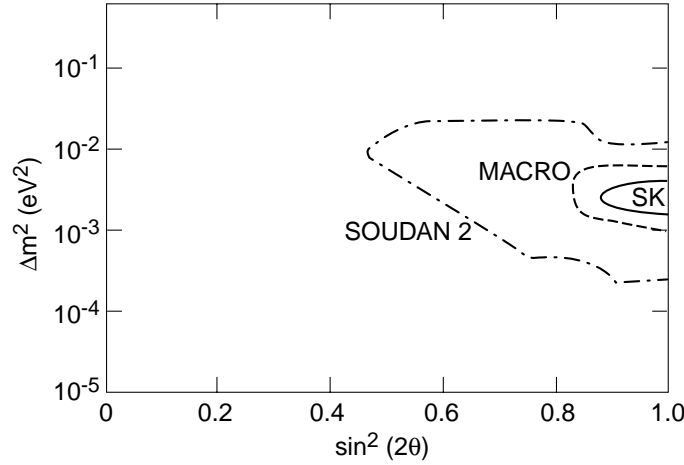


Figure 6: 90% C.L. allowed region contours for  $\nu_\mu \longleftrightarrow \nu_\tau$  oscillations obtained by the SuperKamiokande, MACRO and Soudan 2 experiments.

energy loss calculation in standard rock [15].

The systematic uncertainty arising from the neutrino flux, cross section and muon propagation on the expected flux of upthroughgoing muons was estimated to be  $\sim 17\%$ . This systematic uncertainty is mainly a scale error that doesn't affect the shape of the angular distribution. The same cuts applied to the data were used for the simulated events: they selected 1122 MC events, assuming no oscillations.

Fig: 5a shows the zenith angle ( $\Theta$ ) distribution of the measured flux of upthroughgoing muons of energy  $E_\mu > 1$  GeV (black points); the MC expectation for no oscillations is indicated by the dashed line with the shaded scale error band. A deficit of events in the region around the vertical can be noticed. The ratio of the observed number of events to the expectation without oscillations in  $-1 < \cos \Theta < 0$  ( $\Theta$  is the zenith angle) is  $0.721 \pm 0.026_{stat} \pm 0.043_{sys} \pm 0.123_{th}$ .

We tested the shape of the angular distribution with the hypothesis of no oscillations normalizing the prediction to the data. The  $\chi^2/D.o.F.$  corresponds to a probability of 0.2%. In the hypothesis of only  $\nu_\mu \longleftrightarrow \nu_\tau$  oscillations, the minimum  $\chi^2/D.o.F.$  in the physical region is 9.7/9 ( $P = 37\%$ ) for maximal mixing and  $\Delta m^2 = 2.5 \cdot 10^{-3}$  eV<sup>2</sup>. An independent test was made on the number of the events.

Combining the probabilities from the two independent tests on the zenith angle shape of the flux and on the total number of events, the maximal probability is 66% for maximum mixing and  $\Delta m^2 \simeq 2.4 \cdot 10^{-3}$  eV<sup>2</sup>. The result of the fit is the solid line in Fig: 5a.

For each bin of Fig: 5a we computed the ratio  $R = (\text{measured muon flux})/(\text{expected muon flux in the non oscillation hypothesis})$ . The result is shown in Fig: 5b (black points). The solid line is the ratio  $R$  for maximal mixing and  $\Delta m^2 = 2.5 \cdot 10^{-3}$  eV<sup>2</sup>; the dashed line is the same ratio expected for no oscillations.

The MACRO upthroughgoing muons are very sensitive to oscillations because of the energy range covered. The MACRO 90% C.L. allowed region in the  $\Delta m^2 - \sin^2 2\theta$  plane, computed using the Feldman-Cousins method [16], is smaller than the SuperKamiokande (SK) one for upthroughgoing muons due to the different energy thresholds ( $\sim 1$  GeV for MACRO and  $\sim 6$  GeV for SK) and for the median energies ( $\sim 50$  GeV for MACRO,  $70 \div 80$  GeV for SK).

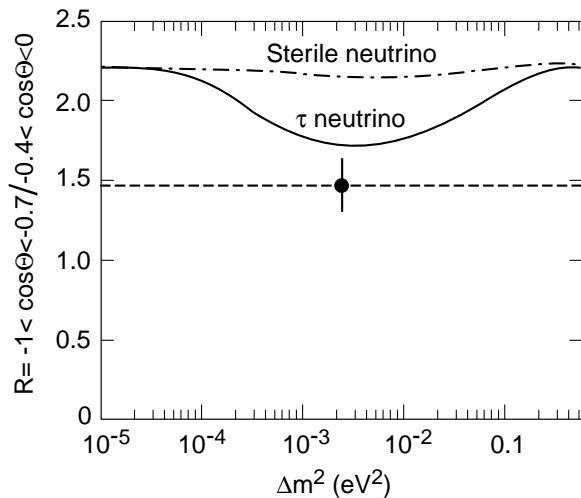


Figure 7: Ratio of events with  $-1 < \cos \Theta < -0.7$  to events with  $-0.4 < \cos \Theta < 0$  as a function of  $\Delta m^2$  for maximal mixing. The black point with error bar is the measured value, the solid line is the prediction for  $\nu_\mu \longleftrightarrow \nu_\tau$  oscillations, the dotted line is the prediction for  $\nu_\mu \longleftrightarrow \nu_{sterile}$  oscillations.

The MACRO 90% C.L. allowed region for  $\nu_\mu \longleftrightarrow \nu_\tau$  oscillations is compared in Fig: 6 with those obtained by the SK and Soudan 2 experiments.

## 5 Matter effects. $\nu_\mu \longleftrightarrow \nu_\tau$ against $\nu_\mu \longleftrightarrow \nu_{sterile}$

Matter effects due to the difference between the weak interaction effective potential for muon neutrinos with respect to sterile neutrinos (which have null potential) would produce a different total number and a different zenith distribution of upgoing muons.

In Fig: 7 the measured ratio between the events with  $-1 < \cos \Theta < -0.7$  and the events with  $-0.4 < \cos \Theta < 0$  is shown by the black point. In this ratio most of the theoretical uncertainties on neutrino flux and cross sections cancel. The remaining theoretical error, estimated at  $\leq 5\%$ , has a 3% contribution due to uncertainties on the kaon/pion fraction produced in atmospheric showers, a 2% contribution from uncertainties in the cross sections of almost vertical and almost horizontal events and a 2.5% contribution from the seasonal variations of the ratio. The systematic experimental error on the ratio, due to analysis cuts and detector efficiencies, is 4.6%. Combining the experimental and theoretical errors in quadrature, a global estimate of 7% is obtained. MACRO measured 305 events with  $-1 < \cos \Theta < -0.7$  and 206 with  $-0.4 < \cos \Theta < 0$ ; the ratio is  $R = 1.48 \pm 0.13_{stat} \pm 0.10_{sys}$ . For  $\Delta m^2 = 2.5 \cdot 10^{-3} \text{ eV}^2$  and maximal mixing, the minimum expected value of the ratio for  $\nu_\mu \longleftrightarrow \nu_\tau$  oscillations is  $R_\tau = 1.72$ ; for  $\nu_\mu \longleftrightarrow \nu_{sterile}$  oscillations one expects  $R_{sterile} = 2.16$ . The maximum probabilities  $P_{best}$  to find a value of  $R_\tau$  and of  $R_{sterile}$  smaller than  $R_{expected}$  are 9.4% and 0.06% respectively. Hence the ratio of the maximum probabilities is  $P_{best_\tau} / P_{best_{sterile}} = 157$ , so that  $\nu_\mu \longleftrightarrow \nu_{sterile}$  oscillations (with any mixing) are excluded at 99% C.L. compared to the  $\nu_\mu \longleftrightarrow \nu_\tau$  channel with maximal mixing and  $\Delta m^2 = 2.5 \cdot 10^{-3} \text{ eV}^2$ .



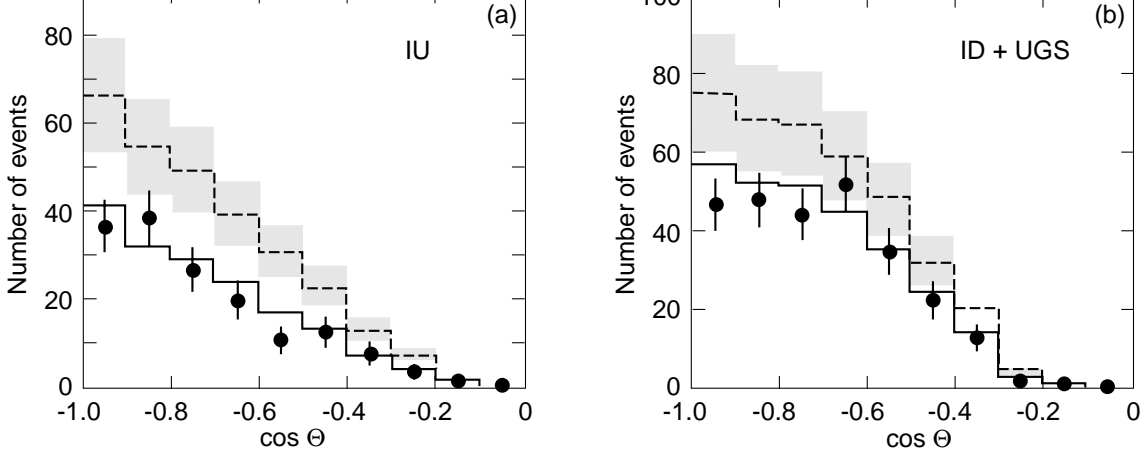


Figure 8: Measured zenith distributions (a) for the IU events and (b) for the ID+UGS events. The black points are the data, the shaded regions correspond to MC predictions assuming no oscillations. The full line is the expectation for  $\nu_\mu \longleftrightarrow \nu_\tau$  oscillations with maximal mixing and  $\Delta m^2 = 2.5 \times 10^{-3} \text{ eV}^2$ .

## 6 Low energy events

The data concern only the running period with the detector in the full configuration from April 1994 to December 2000. During this period more than 40 million downgoing muons were collected. Because of the difference between the topologies of the low energy events, two separate analyses were performed.

The IU sample corresponds to an effective livetime of 5.8 yrs. The basic request is the presence of a streamer tube track reconstructed in space matching at least two hits in two different scintillators in the upper part of the apparatus. The measured muon velocity  $\beta c$  was evaluated with the sign convention that upgoing (downgoing) muons have  $1/\beta \sim -1$  ( $\sim +1$ ). After background subtraction, we had 154 upgoing partially contained events.

The identification of ID+UGS events was based on topological criteria. The candidates had a track starting (ending) in the lower apparatus and crossing the bottom detector face. The track has also to be located or oriented in such a way that it could not have entered (exited) undetected through insensitive regions of the apparatus. For this analysis the effective livetime was 5.6 yrs. After background subtraction, we had 262 ID+UGS events.

The MC simulations for the low energy data use the Bartol neutrino flux [13] and the low energy neutrino cross sections [17]. We estimated a total theoretical scale uncertainty on the predicted number of muons of the order of 25% (it is very probably overestimated).

With the full MC simulation, the prediction for IU events was  $285 \pm 28_{\text{sys}} \pm 71_{\text{th}}$ , while the observed number of events was  $154 \pm 12_{\text{stat}}$ . The ratio was  $R_{IU} = (\text{Data/MC})_{IU} = 0.54 \pm 0.04_{\text{stat}} \pm 0.05_{\text{sys}} \pm 0.13_{\text{th}}$ .

The prediction for ID+UGS events was  $375 \pm 37_{\text{sys}} \pm 94_{\text{th}}$ , while the observed number of events was  $262 \pm 16_{\text{stat}}$ . The ratio was  $R_{ID+UGS} = (\text{Data/MC})_{ID+UGS} = 0.70 \pm 0.04_{\text{stat}} \pm 0.07_{\text{sys}} \pm 0.17_{\text{th}}$ .

The numbers of low energy events are compared with the predictions in Table: 1; the angular distributions are shown in Fig: 8. The data show a uniform deficit of the measured number of events over the whole angular distribution with respect to the predictions without oscillations. The two data sets are consistent with neutrino oscillations with the parameters found in the analysis of the high energy sample. Upgoing neutrinos which induce IU and

Table 1: Summary of the MACRO muon events in  $-1 < \cos \Theta < 0$  after background subtraction. For each topology the number of measured events, the MC prediction for no oscillations and the ratio  $R = (\text{Data}/\text{MC}_{\text{no osc}})$  are given.

	Events	MC <sub>no osc</sub>	$R = (\text{Data}/\text{MC}_{\text{no osc}})$
Upthroughgoing	809	$1122 \pm 191$	$0.721 \pm 0.026_{\text{stat}} \pm 0.043_{\text{sys}} \pm 0.123_{\text{th}}$
IU	154	$285 \pm 28_{\text{sys}} \pm 71_{\text{th}}$	$0.54 \pm 0.04_{\text{stat}} \pm 0.05_{\text{sys}} \pm 0.13_{\text{th}}$
ID+UGS	262	$375 \pm 37_{\text{sys}} \pm 94_{\text{th}}$	$0.70 \pm 0.04_{\text{stat}} \pm 0.07_{\text{sys}} \pm 0.17_{\text{th}}$

UGS events, travelling thousands of kilometers, are reduced by 50%, while no reduction is expected for downgoing partially contained muons. As a rough prediction, we expect a rate reduced by 50% for IU and by 25% for ID+UGS.

The measured data are in good agreement with the predicted angular distributions based on  $\nu_\mu \longleftrightarrow \nu_\tau$  oscillations with the parameters obtained from the upthroughgoing muon sample (full histogram in Fig: 8).

## 7 $\nu_\mu$ energy estimates by Multiple Coulomb Scattering of upthroughgoing muons

Since MACRO was not equipped with a magnet, the only way to experimentally estimate the muon energy is through Multiple Coulomb Scattering (MCS) of muons in the absorbers in the lower part of MACRO, see Fig: 3a. The projected displacement of a relativistic muon with energy  $E_\mu$  travelling for a distance  $X$  can be written as:

$$\sigma_{MCS} \simeq \frac{X}{\sqrt{3}} \frac{13.6 \cdot 10^{-3} \text{GeV}}{p\beta c} \sqrt{X/X^0} \cdot (1 + 0.038 \ln(X/X^0)) \quad (5)$$

where  $p$  (GeV/c) is the muon momentum and  $X/X^0$  is the amount of crossed material in units of radiation lengths. A muon crossing the whole apparatus on the vertical has  $\sigma_{MCS} \simeq 10(\text{cm})/E(\text{GeV})$ . The muon energy estimate can be performed up to a saturation point, occurring when  $\sigma_{MCS}$  is comparable with the detector space resolution.

Two analyses were performed.

The first analysis was made studying the deflection of upthroughgoing muons in MACRO with the streamer tubes in digital mode. Using MC methods to estimate the muon energy from its scattering angle, the data were divided into 3 subsamples with different average energies, in 2 samples in zenith angle  $\Theta$  and finally in 5 subsamples with different average values of  $L/E_\nu$ . This method could reach a spatial resolution of  $\sim 1$  cm. This analysis yielded an  $L/E_\nu$  distribution quite compatible with neutrino oscillations with the parameters found in Section 4.

As the interesting energy region for atmospheric neutrino oscillations spans from  $\sim 1$  GeV to some tens of GeV, it is important to improve the spatial resolution of the detector to push the saturation point as high as possible. For this purpose, a second analysis was performed using the streamer tubes in “drift mode”; the time information was given by a TDC with a bin size of 150 ns. For each triggered tube, the arrival time of the signal multiplied by the drift velocity computed by MC methods ( $\simeq 4$  cm/ $\mu\text{s}$ ) gives the radius of the drift circle. The upthroughgoing muon tracks were reconstructed as the best fit of the drift circles referring to the triggered streamer tubes. The space resolution achieved is  $\simeq 3$

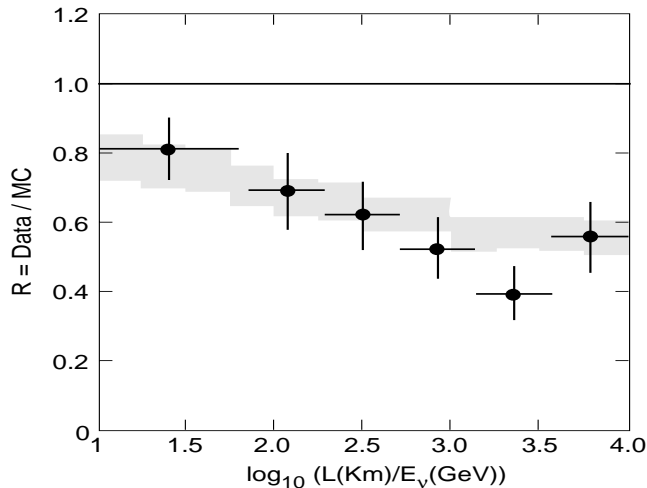


Figure 9:  $R = (\text{Data}/\text{MC}_{\text{no osc}})$  as a function of  $\log_{10}(L/E_\nu)$  obtained using the streamer tubes in “drift mode”. The data are the points with error bars, the line at  $R = 1$  is the prediction for no oscillations; the averages of the shaded region are the predictions for  $\nu_\mu \longleftrightarrow \nu_\tau$  oscillations; the vertical extent of the shaded region represents the MC global uncertainty.

mm, a factor of 3.5 better than in the previous analysis. For each muon, 7 MCS sensitive variables were given in input to a Neural Network (NN) which was previously trained with MC events of known input energy crossing the detector at different zenith angles. The NN output allows to separate the whole sample of upthroughgoing muons in 4 subsamples with average energies  $E_\mu$  of 12, 20, 50 and 102 GeV, respectively. The comparison of the zenith angle distributions of the 4 energy subsamples with the predictions of no oscillations MC shows a strong disagreement at low energies (where there is a deficit of vertical events), while the agreement is restored at higher neutrino energies. The corresponding  $\chi^2$  probabilities for the no oscillation hypothesis in these energy windows are 1.8%, 16.8%, 26.9% and 87.7%, respectively.

The distribution of the ratios  $R = (\text{Data}/\text{MC}_{\text{no osc}})$  obtained by the second method as a function of  $\log_{10}(L/E_\nu)$  is plotted in Fig: 9. The points with error bars are the data; the solid line at  $R = 1$  corresponds to no oscillations; the averages of the shaded area are the MC predictions for  $\nu_\mu \longleftrightarrow \nu_\tau$  oscillations with maximal mixing and  $\Delta m^2 = 2.5 \times 10^{-3} \text{ eV}^2$ ; the vertical extent of the shaded area represents the MC global uncertainty.

The 90% C.L. allowed region obtained with this analysis is consistent with the MACRO region plotted in Fig: 6.

The semicontained data yielded another point at  $\log_{10}(L/E_\nu) \simeq 3.2$  which is consistent with neutrino oscillations.

## 8 Conclusions

We presented and discussed the MACRO results on atmospheric neutrinos. The measured and expected numbers of events are summarized in Table: 1. The observed zenith angle distributions and the numbers of neutrino-induced muons (Fig: 5 and Fig: 8) disagree with the predictions of the no oscillation hypothesis. The muon angular distribution and flux are in agreement with the hypothesis of two flavour  $\nu_\mu \longleftrightarrow \nu_\tau$  oscillations, with maximal mixing

and  $\Delta m^2_{21}$  are  $\sim 10^{-5} \text{ eV}^2$ . The hypothesis of  $\nu_\mu \leftrightarrow \nu_\tau$  sterile oscillation is disfavored at the 99% C.L. The MACRO 90% C.L. contours in the plane  $\Delta m^2 - \sin^2 2\theta$  are compared in Fig. 6 with those obtained by the Soudan 2 and SuperKamiokande experiments: they overlap closely. The data from the three experiments strongly favour  $\nu_\mu \longleftrightarrow \nu_\tau$  oscillations, though other possible interpretations have been suggested, see for example ref. [18].

Other MACRO results in the field of neutrino physics and astrophysics concern: (i) the search for cosmic point sources of high energy muon neutrinos: the flux upper limits for many sources, like Vela P, are at the level of  $\Phi_\nu \sim 2 \cdot 10^{-6} \text{ cm}^{-2} \text{ s}^{-1}$  [19]; (ii) the search for dark matter WIMPs annihilating and yielding muon neutrinos from the earth core and from the Sun: the measured flux upper limits exclude ranges of parameters of supersymmetric models [20]; (iii) the search for low energy  $\bar{\nu}_e$  from stellar gravitational collapses: from 1989 till 2000 no type II supernovae exploded in our galaxy [21].

## 9 Acknowledgements

We acknowledge the cooperation of many members of the MACRO Collaboration, in particular of D. Bakari, Y. Becherini, P. Bernardini, T. Montaruli, F. Ronga, E. Scapparone, M. Sioli, M. Spurio, A. Surdo.

## References

- [1] G. Barr et al., *Phys. Rev.* **D39** (1989) 3532; M. Honda et al., *Phys. Lett.* **B248** (1990) 193; H. Lee and Y.S. Koh, *Nuovo Cimento* **105B** (1990) 883.
- [2] L.V. Volkova, *Sov. J. Nucl. Phys.* **31** (1980) 784; K. Mitsui et al., *Nuovo Cimento* **9C** (1986) 995; A.V. Butkevich et al., *Sov. J. Nucl. Phys.* **50** (1989) 90.
- [3] IMB Coll., R. Becker-Szendy et al., *Phys. Rev.* **D46** (1992) 3720.
- [4] Kamiokande Coll., Y. Fukuda et al., *Phys. Lett.* **B335** (1994) 237.
- [5] NUSEX Coll., M. Aglietta et al., 23<sup>rd</sup> ICRC Proc., Calgary, Canada, Vol. **4** (1993) 446.
- [6] Frejus Coll., K. Daum et al., *Z. Phys.* **C66** (1995) 417.
- [7] Baksan Coll., S. Mikheyev, 5<sup>th</sup> TAUP Workshop Proc., Gran Sasso, Italy, 1997.
- [8] Soudan 2 Coll., W.W.M. Allison et al., *Phys. Lett.* **B391** (1997) 491; *Phys. Lett.* **B449** (1999) 137; W. Anthony Mann, hep-ex/0007031.
- [9] MACRO Coll., S. Ahlen et al., *Phys. Lett.* **B357**(1995) 481. MACRO Coll., M. Ambrosio et al., *Phys. Lett.* **B434** (1998) 451; *Phys. Lett.* **B478** (2000) 5; *Phys. Lett.* **B517** (2001) 59.
- [10] SuperKamiokande Coll., Y.Fukuda et al., *Phys. Rev. Lett.* **81** (1998) 1562; *Phys. Lett.* **B433** (1998) 9; *Phys. Rev. Lett.* **85** (2000) 3999; *Nucl Phys. B Proc. Suppl.* **91** (2001) 127; T. Toshito, hep-ex/0105023 (2001).
- [11] MACRO Coll., M. Ambrosio et al., *The MACRO detector at Gran Sasso*, accepted for publication on *Nucl. Instr. Meth. A*.
- [12] MACRO Coll., M. Ambrosio et al., *Astrop. Phys.* **9** (1998) 123.

- [13] W. H. Ng and S. Pak, *Phys. Rev. D* **33** (1986) 1511.
- [14] M. Gluck et al., *Z. Phys.* **C67** (1995) 433.
- [15] W. Lohmann et al., *Energy loss of muons in the energy range 1-GeV to 10000-GeV.*, CERN-EP/85-03 (1985).
- [16] G.J. Feldman and R.D. Cousins, *Phys. Rev.* **D57** (1998) 3873.
- [17] P. Lipari et al., *Phys. Rev. Lett.* **74** (1995) 4384.
- [18] V. Popa and M. Rujoiu, *Exotic neutrino oscillations*, to be published in the Proc. of the NATO ARW, Oujda, Morocco, (2001).
- [19] MACRO Coll., M. Ambrosio et al., *ApJ.* **546** (2001) 1038.
- [20] MACRO Coll., M. Ambrosio et al., *Phys. Rev.* **D60** (1999) 082002.
- [21] MACRO Coll., M. Ambrosio et al., *Astrop. Phys.* **8** (1998) 123.